

---

# Narrowing the Focus: Learned Optimizers for Pretrained Models

---

**Gus Kristiansen\***  
Google DeepMind

**Mark Sandler**  
Google DeepMind

**Andrey Zhmoginov**  
Google DeepMind

**Nolan Miller** Google DeepMind    **Anirudh Goyal** Mila – Quebec AI Institute    **Jihwan Lee** Google DeepMind    **Max Vladymyrov\*** Google DeepMind

## Abstract

In modern deep learning, the models are learned by applying gradient updates using an optimizer, which transforms the updates based on various statistics. Optimizers are often hand-designed and tuning their hyperparameters is a big part of the training process. Learned optimizers have shown some initial promise, but are generally unsuccessful as a general optimization mechanism applicable to every problem. In this work we explore a different direction: instead of learning general optimizers, we instead specialize them to a specific training environment. We propose a novel optimizer technique that learns a layer-specific linear combination of update directions provided by a set of base optimizers, effectively adapting its strategy to the specific model and dataset. When evaluated on image classification tasks, this specialized optimizer significantly outperforms both traditional off-the-shelf methods such as Adam, as well as existing general learned optimizers. Moreover, it demonstrates robust generalization with respect to model initialization, evaluating on unseen datasets, and training durations beyond its meta-training horizon.

## 1 Introduction

The optimization loop forms the backbone of machine learning algorithms. The choice of optimizer and its hyperparameters heavily influences the final model’s performance. Despite its importance, optimizer selection often relies on heuristics and domain-specific knowledge. For instance, Adam optimizer (Kingma & Ba, 2014) excels with language problems, but struggles with image classification problems. The potential of second-order methods for stochastic data remains largely untapped, except for a few notable exceptions (Martens & Grosse, 2015; Gupta et al., 2018). Every year, more and more optimization methods are proposed, making it increasingly challenging for practitioner to select the best one (Choi et al., 2019; Schmidt et al., 2021).

Learned optimizers or learning-to-learn methods (Schmidhuber, 1987; Bengio et al., 1990, 2013) offer a potential solution to this challenge by automating the optimizer selection process. These methods automate this process by either learning the hyperparameters of existing optimizers or developing entirely new optimization algorithms. However, two significant challenges limit widespread adoption of learned optimizers: meta-optimization difficulties, and meta-generalization.

Meta-optimization difficulties arise from the sensitivity of gradients in bi-level optimization with a high number of training iterations (aka optimization horizon) (Metz et al., 2021). Evolutionary methods can help mitigate this because they do not rely directly on gradients, and thus are less susceptible to gradient sensitivity issues. However, the complexity of the problem increases with

---

\*Correspondence to [gusatb@google.com](mailto:gusatb@google.com), [mxv@google.com](mailto:mxv@google.com)

the length of the optimization horizon. Short horizon bias (Wu et al., 2018) constitutes another problem, where meta-optimization over a specified time horizon introduces a bias that prevents it to be applicable to a longer time horizon.

Meta-generalization refers to a learned optimizer’s ability to perform well on novel tasks it was not specifically trained for. One approach to achieving this is to train the optimizer on the widest possible range of tasks. Previous research focused on developing a single, adaptable algorithm by training it on a very broad domain. For example, Versatile Learned Optimizers (VELO, Metz et al., 2022) was trained on hundreds of different problems, ranging from simple linear regression to reinforcement learning. However, this “one-size-fits-all” approach has significant drawbacks. The computational cost of training such an optimizer is immense, requiring 4 000 TPU-months in the case of VELO. Furthermore, a single optimizer struggles to effectively adapt to the vast array of loss surfaces encountered across such a diverse set of tasks. This makes it challenging to achieve consistently high performance across all tasks.

Instead of aiming for broad applicability, we focus on the increasingly relevant domain of fine-tuning pretrained models. This specialization allows us to develop learned optimizers in a more targeted way. By narrowing the scope of the meta-training domain, the learned optimizer can specialize and excel in the specific types of tasks it is designed for. Fine-tuning also simplifies the optimization problem by leveraging existing knowledge encoded in pretrained checkpoints (Wei et al., 2021) and is typically done for a relatively few iterations, since only a small alignment with the current task is needed to achieve a good result.

To achieve this, we introduce L3RS (Learned Layer-wise Learning Rate Scheduler, pronounced “lers”), a novel learned optimizer designed specifically to leverage the performance of a set of predefined base optimizers within a narrower domain. L3RS uses a variety of performance features, such as adaptive exponential moving averages (EMA) across different scales. EMAs, or model averaging, have demonstrated improved generalization in real-world applications (Tsvaini & Valpola, 2017; Izmailov et al., 2018). Based on these features, L3RS produces layer-wise updates as a linear combination of the predefined base optimizers, along with a corresponding learning rate for each layer.

Our contributions are as follows.

- We propose a novel learning-to-learn method that leverages the strengths of multiple base optimization methods. This optimizer is simple and intuitive, having only a fraction of parameters compared to other black-box learned optimizers.
- We demonstrate that meta-training a learned optimizer on a narrow domain results in an optimizer that can outperform existing methods, with more than 50% speedup compared to another learned optimizer baseline, and more than  $2 \times$  speedup compared to best performing traditional optimizers.
- We evaluate the meta-generalization of the proposed optimizer across several components: generalization to longer training horizon, different pretraining and model initializations, and different evaluation dataset.

## 2 Preliminaries

Consider a loss function  $L(\theta, X)$ , parameterized by  $\theta$  for a given data  $X$ . Learned optimizers  $f_\psi$ , parameterized by  $\psi$ , provide a direction to update the model’s weights  $\theta$  as

$$\theta_{n+1} = \theta_n + f_\psi(\Phi; \theta_n, X), \quad (1)$$

where  $\Phi$  is a collection of features that describes the current (or past) optimization statistics, such as the gradient or the loss value. For example, the simplest learned optimizer might simply optimize the learning rate  $\lambda$  of SGD, as  $f_\psi(\Phi; \theta_n, X) = \lambda \nabla L(\theta_n, X)$ , in which case  $\Phi := \{\nabla L\}$  and  $\psi := \{\lambda\}$ . In case of ADAM, the optimization parameters would be  $\psi := \{\lambda, \beta_1, \beta_2\}$ .

In Figure 1 we show both the inner and the outer loop of a typical meta-training process. We train  $\psi$  on a distribution of tasks from a given dataset. A task is a set  $T := \{\theta_0, \{D_K^t\}, D^e\}$ , where  $\theta_0$  represents initial model weights (or a distribution of initial model weights),  $\{D_K^t\}$  is a sequence of

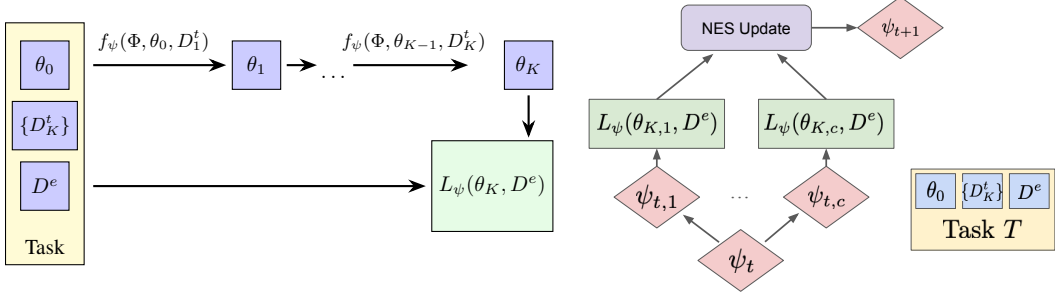


Figure 1: *Left:* Inner loop evaluation. Given a task  $T := \{\theta_0, \{D_K^t\}, D^e\}$ , the learned optimizer  $f_\psi$  uses optimization statistics  $\Phi$  to update model parameters starting from  $\theta_0$  for each of  $\{D_K^t\}$  batches. After  $K$  update steps, the final model parameters are evaluated on the evaluation set  $D^e$  using meta-loss  $L_\psi$ . *Right:* Outer loop NES meta-training iteration. Given a task  $T$  and meta-parameters  $\psi_T$ , Gaussian noise is added to  $\psi_t$  to produce a number of candidates equal to the population size  $c$ ,  $(\psi_{t,0}, \dots, \psi_{t,c})$ . An inner loop evaluation is performed on the given task for all candidates. The fitness of each candidate is then used to perform an NES update step, resulting in the next learned optimizer parameters,  $\psi_{t+1}$ .

$K$  training batches, and  $D^e$  represents an evaluation batch. A batch typically consists of data  $X$  and, for classification problems, may also include labels. We assume that  $\theta_0$  is given as input, and we have no control over its generation process (unlike initialization-based meta-learning approaches, such as MAML, Finn et al., 2017).

Learned optimizer parameters  $\psi$  are evaluated by performing  $K$  update steps (1) on every batch from  $D_K^t$ , to get  $\theta_K$  and calculating the loss using the evaluation batch  $L_\psi(\theta_K, D^e)$ .

We use Natural Evolution Strategies (NES, Salimans et al., 2017) to meta-train the learned optimizers. We define a task meta-loss  $L_\psi^M(T) = L_\psi(\theta_K, D^e)$ , the loss on the evaluation batch after  $K$  training steps of a task  $T = \{\theta_0, \{D_K^t\}, D^e\}$ . We then define a fitness function  $F(\psi, (T_1, \dots, T_b)) = -\frac{1}{b} \sum_{i=1}^b L_\psi^M(T_i)$ , using a batch of  $b$  tasks for each generation. NES is used to maximize the fitness function during meta-training.

After the learned optimizer is trained, it can be evaluated to a new task distribution  $\tilde{T} := \{\tilde{\theta}_0, \{\tilde{D}_K^t\}, \tilde{D}^e\}$ .

### 3 Motivation and Related Work

We can separate the optimizers into two main categories. First category, so called black-box optimizers (Li & Malik, 2016; Andrychowicz et al., 2016; Wichrowska et al., 2017; Lv et al., 2017; Sandler et al., 2021; Metz et al., 2020a,b, 2022), learns an update function  $f_\psi$  from scratch using a custom inner optimization loop. These methods often have a large number of parameters, making them prone to overfitting and stability issues (Harrison et al., 2022). While recent work has explored using Transformers as a meta-learner architecture (Chen et al., 2022; Moudgil et al., 2023; Jain et al., 2024), they have not yet shown a significant advantage over traditional optimizers or other learned optimizer architectures.

A notable example of black-box optimizer is VELLO, which uses per-tensor HyperNetworks (Ha et al., 2016) represented by 512-wide LSTMs to generate parameters of per-parameter MLPs. To compute the parameter updates, it passes the per-parameter features through the generated MLP network consisting of 2-hidden layer, 4-hidden MLP. The input to the HyperNetwork and MLP vary slightly, but generally represent the training dynamic of the optimization. VELLO is designed to be general and has a lot of parameters that need to be learned, which makes meta-training very expensive. We envision an ideal optimizer would be lean and ideally fast to train on a narrow task domain.

Other techniques utilize algorithm discovery as a program search (Bello et al., 2017; Wang et al., 2022; Zheng et al., 2022; Chen et al., 2023), where the symbolic optimizers are found using a tree search of predefined operations (such as gradient and momentum).

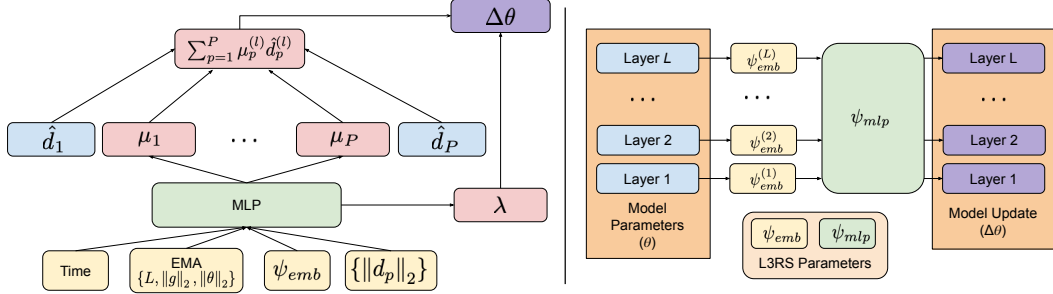


Figure 2: Left: L3RS applied to a single layer of the target model. The MLP receives the norm of each direction provided, time features, target layer embedding, and EMA features of the global loss, layer gradient norm and layer parameter norm. The MLP outputs the weighting for each direction ( $\mu_p$ ) as well as the final update norm ( $\lambda$ ). Right: L3RS is applied at every layer of the network independently with the same MLP weights but different layer embeddings.

The second category of meta-optimizers learns a higher-level meta-component on top of existing hand-designed optimizers. Such approaches include learning to adapt the hyperparameters of an underlying optimizer Daniel et al. (2016), or learn a schedule for the learning rate (Xu et al., 2017, 2019). In addition, these methods can include adapting the optimizer’s parameters directly (Shaban et al., 2019). Hypergradient methods (Maclaurin et al., 2015; Baydin et al., 2017; Grazzi et al., 2020; Moskovitz et al., 2019) perform a hyperparameter search on-the-fly during optimization.

Our proposed approach strikes a balance between flexibility of black-box minimizer and the stability of learning hyperparameters of known optimizers. We leverage the benefits of hand-designed optimizers while incorporating the adaptability of learned components using a simple small neural network for learning the per-layer learning rate. Unlike existing methods that learn a fixed set of hyperparameters for a single existing optimizer, L3RS learns from a set of base-optimizers. Moreover, during meta-training we also search over the hyperparameters of the base-optimizer.

Almeida et al. (2021) is probably the closest algorithm to our setting. It uses an LSTM controller to adjust the hyperparameters of a hand-designed inner-optimizer, which uses a collection of hand-designed parts from different known optimizers. A major difference with our method is that L3RS operates per-layer and that our algorithm wraps existing optimizers out-of-the box, without the need to manually add features.

Prémont-Schwarz et al. (2022) also propose an in-between approach, where the learned optimizer falls back to the base-optimizer. However, their goal was to ensure convergence, not necessarily to improve the performance.

The L3RS architecture was also partially motivated by Learning Rate Grafting (Agarwal et al., 2022), which demonstrates the utility of isolating the direction of an optimizer from its magnitude.

Similar to our paper Landro et al. (2021) also propose an algorithm that combines Adam and SGD as a linear combination of their update direction. However, their method differs significantly in two key aspects: (1) they do not provide a mechanism for learning the mixing coefficient, instead treating it as fixed hyperparameters, and (2) their combination is applied globally across all layers, while our proposed method, L3RS, employs a layer-wise adaptive strategy.

## 4 L3RS: Learned Layer-wise Learning Rate Scheduler

### 4.1 Model architecture

Given a set of update vectors  $d_p$  from  $P$  input base optimizers (e.g. SGD or Adam) L3RS computes a model parameter update step per layer  $l$  using:

$$\Delta\theta^{(l)} = \lambda^{(l)} \sum_{p=1}^P \mu_p^{(l)} \hat{d}_p^{(l)}, \quad (2)$$

where  $\lambda^{(l)}$  is a layer-specific update  $l_2$ -norm,  $\mu_p^{(l)}$  are normalized mixing coefficients for the base optimizers' directions  $\sum_{p=1}^P \mu_p^{(l)} = 1$ , and  $\hat{d}_p^{(l)}$  are normalized optimizers' direction  $\hat{d}_p^{(l)} = \frac{d_p^{(l)}}{\|d_p^{(l)}\|_2}$ .

Figure 2 shows the main input and output components of L3RS as well as provide a flow-chart on how the weights of the underlying model  $\theta$  are updated.

In order to learn  $\lambda^{(l)}$  and  $\mu_p^{(l)}$ , we provide L3RS with a feature vector, comprising the adaptive EMA, time, embedding features as well as the magnitude of the update directions defined below. This input is then processed by two fully connected layers with sizes 32 and 16, using ReLU activation. The model outputs logits  $z^{(l)} \in \mathbb{R}^{P+1}$ , from which we reconstruct  $\mu_p^{(l)} = \frac{\exp(z_p^{(l)})}{\sum_{j=1}^P \exp(z_j^{(l)})}$  and  $\lambda^{(l)} = \exp(z_{P+1}^{(l)})$ .

The hyperparameters of the input optimizer (e.g. Adam's  $\beta_1$  and  $\beta_2$ ) are also jointly meta-learned along with the L3RS's model parameters. This enables co-adaptation of the layer-wise scaling and the underlying optimization algorithm.

**Adaptive Exponential Moving Averages (EMA).** In order to capture both short-term and long-term performance trends, for each layer  $l$ , we maintain four EMAs with different smoothing factors  $\gamma \in \{0, 0.9, 0.99\}$ . EMAs are updated recursively as  $a_{i,k+1}^{(l)} := \gamma_i a_{i,k}^{(l)} + (1 - \gamma_i) \xi^{(l)}$ , where  $a_{i,k}^{(l)}$  denotes the  $i$ th EMA for layer  $l$  at time step  $k$ , and  $\xi^{(l)}$  represents a layer-specific statistic of interest. Specifically, for a given layer we track the following:

- *Log  $l_2$ -norm of weights.*  $\log(\|w^{(l)}\|_2)$ , where  $w^{(l)}$  are the weights for layer  $l$ .
- *Log  $l_2$ -norm of gradients.*  $\log(\|g^{(l)}\|_2)$ , where  $g^{(l)}$  are the gradients for layer  $l$ .
- *Loss.* The loss of the overall model (shared across all layers).

To ensure unbiased estimates, especially during the initial time steps, we apply a bias correction to the EMAs before incorporating them as input features:  $\tilde{a}_k^{(l)} = \frac{a_k^{(l)}}{1 - \gamma^k}$ .

**Time features.** Inspired by VELO (Metz et al., 2022), we propose incorporating the following time features for the explicit modeling of temporal dynamics of the optimization progress. These features enable the optimizer to adapt its strategy based on the stage of the training process. These features are generated using  $k$ , the current training step, and  $K$ , the number of total training steps. Similar to some learning rate schedulers,  $K$  must be given to the optimizer at the beginning of training so that these time features can be generated.

- *Relative time features.*  $\tanh(10(\frac{k}{K} - \alpha_i))$ , where  $\alpha_i$  are 11 linearly scaled reference points between 0.0 and 1.0, inclusive. These features capture the relative progress through a sequence, with the hyperbolic tangent function providing a smooth, bounded representation. Figure 6 in the Appendix shows the values of these features throughout training.
- *Absolute time features.*  $\tanh(\log(K\beta_j))$ , where  $\beta_j$  are 4 log-scaled scaling factors between 0.0001 and 0.1. These features provide a logarithmic encoding of the total duration, which can be useful for appropriate learning rate scaling. For longer time horizons these features can be extended such that  $\max(\beta) > \max(K)$ . Figure 7 in the Appendix shows the values of these features for various total training lengths  $K$ .

**Embedding features.** A 16-dimensional embedding vector  $\psi_{emb}$  is meta-learned for each layer, allowing the optimizer to learn specialized per-layer dynamics.

**Base-optimizer direction magnitude.** For each base optimizer  $d_p$ , the log  $l_2$ -norm of the direction is provided:  $\log(\|d_p\|_2)$ .

## 4.2 Comparison with VELO

VELO was designed with an efficient hypernetwork-style architecture. The majority of the computation cost is reduced to per-layer LSTM networks, which then generate cheaper per-parameter networks which output the update step direction. L3RS is able to leverage smaller MLP networks

Optimizer	State Memory	Update Function Size
SGD	0.0×	61.4 KiB
ADAM	2.0×	240.0 KiB
L3RS	2.0×	2.9 MiB
VELO	4.0×	418.78 MiB

Table 1: Compute and memory costs for various optimizers. State memory is the ratio of the optimizer state size to the model parameter size. Update Function Size is the size of the compiled code to calculate the weight update given the gradients. Target model is ResNet-34 with 1000 classes.

for the per-layer operations, and can rely on base optimizers rather than generating the update step direction manually. These design choices result in a learned optimizer which will typically have two to three orders of magnitude fewer parameters compared to VELO.

## 5 Experiments

To evaluate the performance of our proposed L3RS optimizer, we designed a series of image classification experiments using the ResNet-34 model.

**Model Choices.** While our proposed L3RS can wrap any number of base-optimizers, we found that even a simple version that combines together only ADAM and SGD (without momentum) directions performs well. For the remainder of this paper, when we refer to L3RS, we specifically mean this ADAM and SGD combination unless we specify otherwise.

During inference, the memory footprint of this L3RS optimizer state is  $2 \times$  the model parameters (all from ADAM). VELO uses a memory state of  $4 \times$  the model parameters (plus additional memory from 3 AdaFactor style accumulators). Table 1 shows a comparison of the memory state requirements for various optimizers, as well as the compute cost for each.

We derive updates separately for every convolutional, dense or batch normalization layer of the model, including separate updates for kernels and biases. For ResNet-34, this results in  $L = 111$  components for which we compute learning rate  $\lambda^{(l)}$  and mixing coefficients  $\mu_p^{(l)}$ , for  $l = 1, \dots, L$ . With  $P = 2$  optimizers, L3RS outputs 333 parameters per iteration.

For NES training, we use a smooth exponential decay for both meta-learning rate  $\alpha$  and the Gaussian noise standard deviation  $\sigma$  by 0.5 every 500 generations. We use the same antithetic sampling and fitness transformations as in Salimans et al., 2017. We use a population size of 32, meta-batch size of 4 and train for 2000 generations for all our experiments (except the ablation study). We parallelize the evaluation of each candidate in the population, using a total of 32 A100 GPUs for four days.

**Task Distribution and Meta-Training.** We trained the learned optimizer using IMAGENET dataset in the following way. We partition the IMAGENET dataset into three distinct subsets: pretraining, meta-train (IMAGENET25), and meta-test (IMAGENET25EVAL). The first 500 classes are used to pretrain a model using a conventional off-the-shelf algorithm. The pretrained model serves as an initialization to our method. The remaining 500 classes are randomly divided into meta-train and meta-test sets. Details on checkpoint pretraining are provided in Appendix A.

A task within our meta-learning framework is constructed by randomly sampling 25 classes from either the IMAGENET25 or IMAGENET25EVAL set. The selected classes are used to generate  $K$  training batches with 64 samples each and 1 evaluation batch with 256 samples, using the train and validation splits respectively. During meta-training, the number of training batches  $K$  is uniformly sampled from a range of 10 to 500, simulating diverse fine-tuning scenarios.

We meta-train the L3RS optimizer and the VELO optimizer on the IMAGENET25 meta-train task distribution using NES as described above.

**Meta-Evaluation and Baselines.** To evaluate the performance, we check for in-distribution and out-of-distribution generalization. For *in-distribution evaluation* we use the same initialization as the meta-training ( $\tilde{\theta}_0 = \theta_0$ ) and use IMAGENET25EVAL tasks for meta-test. For *out-of-distribution evaluation* we use the PLACES (López-Cifuentes et al., 2020) dataset. We create a separate PLACES initialization

by pretraining ResNet-34 on the first 150 classes of PLACES. We use the remaining classes as a meta-test set (PLACES25EVAL). Importantly, this dataset is entirely novel and unseen during the meta-training, which allows us to evaluate out-of-distribution performance of the optimizers.

We compare L3RS against the following baselines:

- VELO (ft). An instance of VELO meta-trained using the same method as L3RS.
- VELO (og). The original pretrained VELO model (Metz et al., 2022), representing a general-purpose learned optimizer.
- VELO (og, Head). The original pretrained VELO model applied to only the final model layer (freezing the rest of the model).
- ADAM (cosine). Adam optimizer with a cosine learning rate schedule.
- ADAM (cosine, Head). Adam optimizer with a cosine learning rate schedule applied to only the final model layer (freezing the rest of the model).
- ADAM (const). Adam optimizer with constant learning rate.
- ADAM (const, Head). Adam optimizer with constant learning rate applied to only the final model layer (freezing the rest of the model).

For optimizers which parameters depend on the number of training steps  $K$ , such as ADAM (cosine), VELO (ft) and L3RS, we perform separate evaluations across various  $K$  values to assess their performance both within and beyond the meta-training regime.

For all meta-evaluations we average the results of 100 tasks sampled from the specified task distribution. The average and standard deviation of eval accuracy across the sampled tasks is reported.

**Results.** Figure 3 shows the main result. Our goal is to assess the performance of the learned optimizer under various conditions, for both in and out of distribution scenarios. **(A)** Represents in-distribution evaluation, where the initialization, evaluation dataset, and the number of steps match the meta-training regime. We also explore out-of-distribution performance by extending the number of evaluation steps beyond the meta-training range (indicated by the dashed line in all plots), changing the evaluation dataset to PLACES25EVAL **(B)**, modifying the initialization to utilize a model pretrained on PLACES **(C)**, or using both the PLACES checkpoint and PLACES25EVAL dataset **(D)**.

First, comparing VELO (ft) to VELO (og), we observe that fine-tuning VELO to a specific dataset and number of steps leads to a significant performance improvement compared to the general-purpose VELO (og). However, VELO (ft) performance deteriorates sharply when evaluated outside its meta-training regime. We hypothesize this is due to VELO complexity and parameter count, making it more sensitive to deviations from its training distribution, especially number of steps.

Despite the improvement from fine-tuning, VELO (ft) still underperforms compared to L3RS. We attribute this to L3RS’s more lightweight architecture and its inherent ability to fallback to the performance of its base optimizers for robust performance. L3RS also performs favorably against ADAM for all  $K$  values within the training distribution (10 to 500 steps), but their performance becomes comparable when evaluated beyond  $K = 1000$  steps.

Interestingly, changing either the initialization or evaluation dataset to PLACES has a minimal effect on the relative performance of the optimizers, even though PLACES was not included in the meta-training data. This highlights the robust generalization capabilities of both L3RS and the fine-tuned VELO.

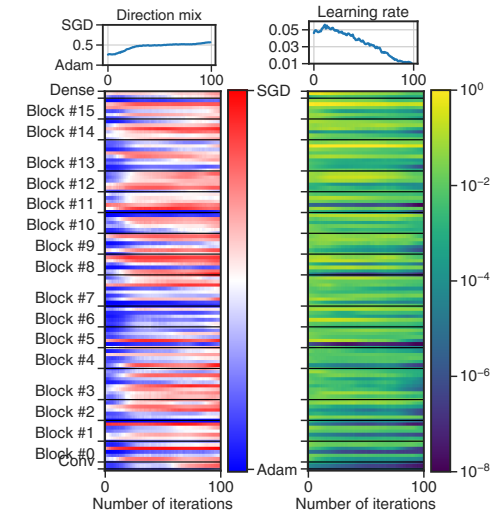


Figure 4: Learned mixing coefficients  $\mu_p^{(l)}$  and  $\lambda^{(l)}$  for each iteration of L3RS for ResNet-34 model. *Top:* average across all the layers. *Bottom:* individual for every learned component.

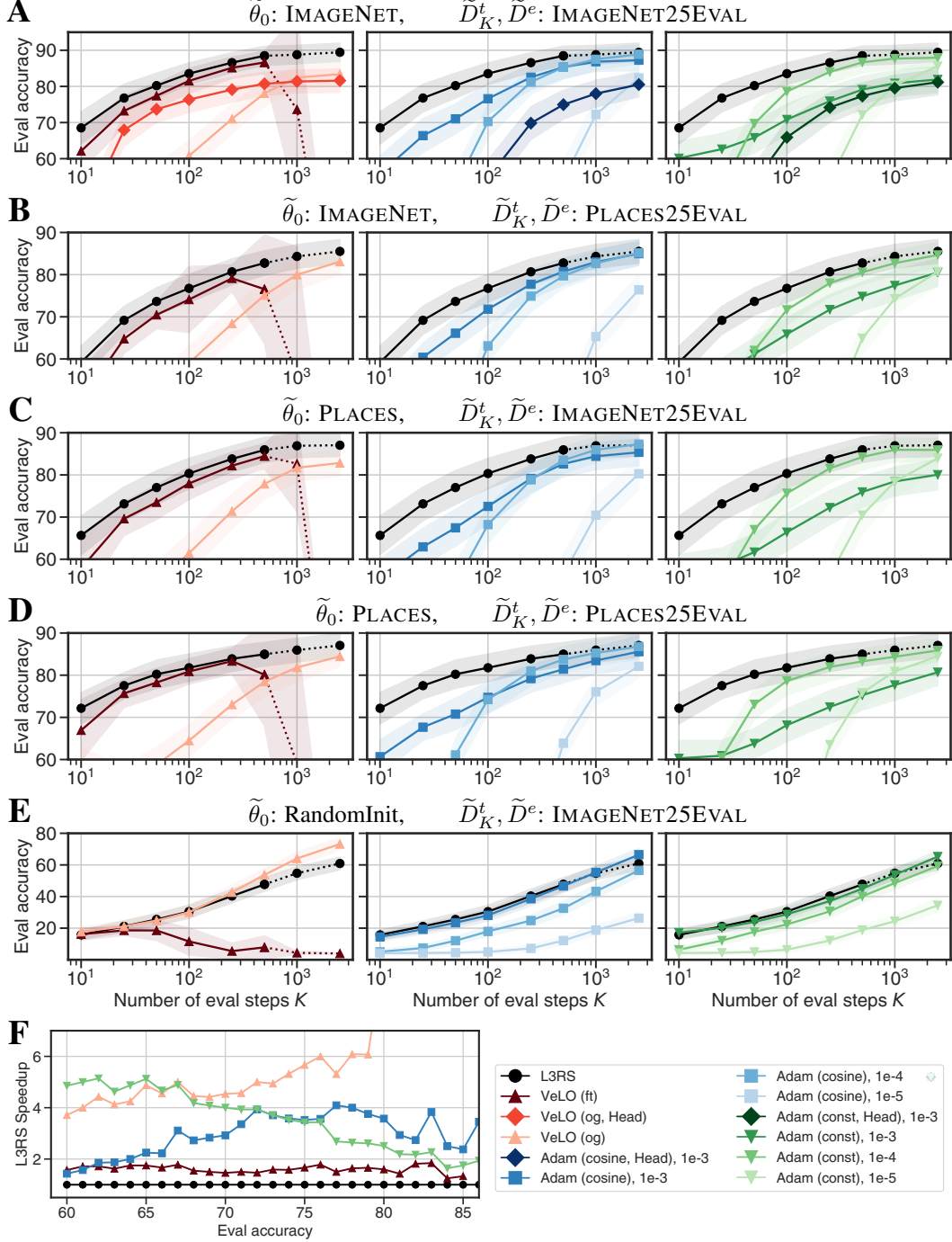


Figure 3: Meta-evaluation of the L3RS, meta-trained on IMAGESET25 for 10 to 500 steps along with various benchmarks. Performance is compared to Velo (left), Adam with cosine learning rate (center), and Adam with a constant learning rate (right). Each marker represents model evaluation at that number of steps. Solid lines indicate the number of steps for in-distribution evaluation, while dashed lines indicate generalization to more steps than meta-training.

- A. **In-domain Generalization.** Both initialization and evaluation are on IMAGESET.
- B. **Out-of-Domain Initialization.** Initialized on IMAGESET, evaluated on PLACES25EVAL.
- C. **Out-of-Domain Evaluation.** Initialized on PLACES, evaluated on IMAGESET25EVAL.
- D. **Out-of-Domain Init & Eval.** Both initialization and evaluation are on PLACES dataset.
- E. **Random Initialization.** Random initialization, evaluated on IMAGESET25EVAL dataset.
- F. **Speedup of L3RS.** For in-domain generalization, this shows how much faster L3RS achieves a given accuracy compared to the baselines.

Base-optimizers	No Embedding	Per-layer MLP	Embedding
SGD only	$64.48 \pm 5.05$	$64.71 \pm 5.00$	$68.18 \pm 4.29$
ADAM only	$61.44 \pm 5.14$	$67.14 \pm 4.57$	$68.52 \pm 4.25$
SGD, ADAM	$65.70 \pm 4.91$	$68.52 \pm 4.40$	<b><math>68.93 \pm 4.58</math></b>

Table 2: Average and standard deviation evaluation accuracy given different optimizers and per-layer strategies.

EMA's Smoothing Factors	Accuracy
$\gamma \in \{0.99, 0.9, 0.0\}$	$68.93 \pm 4.34$
$\gamma \in \{0.9, 0.0\}$	$67.43 \pm 4.64$
$\gamma \in \{0.0\}$	$67.78 \pm 4.47$
$\gamma \in \emptyset$	$66.52 \pm 4.84$

Table 3: Average and standard deviation evaluation accuracy given adaptive EMA features.

We also apply the methods to a randomly initialized Resnet-34 model (**E**). RandomInit uses a standard initialization method (Klambauer et al., 2017). In this case, L3RS does not outperform the baseline methods. We believe this is because, while L3RS generalizes well to different checkpoints (**C**), the randomly initialized model may be too different and far out of distribution for L3RS to perform optimally.

In Figure 3 (**F**) we show the speedup, in training steps, L3RS achieves over baseline methods to reach a given accuracy. L3RS robustly is able to demonstrate 50% speedup over VELO (ft) and 100% speedup over the best hand-designed optimizer.

Finally, Figure 4 shows the learned parameters of L3RS during a 100-step evaluation run. Interestingly, the optimizer initially heavily favors ADAM direction, switching towards SGD as training progresses (with a curious sudden switch for some layers around iteration 10). Moreover, some layers consistently rely on SGD or ADAM direction throughout the entire run. While the precise interpretation of these parameter dynamics is challenging, the parameters of L3RS are considerably more interpretable than those of most black-box learned optimizers.

## 6 Ablations and Variants

We perform a methodical ablation and variant study to justify the design choices of the L3RS architecture. We meta-train all models in this section using the IMAGENET25 task distribution but set number of steps,  $K$ , to 10. We additionally meta-train for 500 generations of NES and change the meta-learning rate decay rate steps from 500 to 100.

**Ablation of Base Optimizers.** We first show the results of using either SGD or ADAM alone as the wrapped optimizer rather than both together.

**Embedding Variants.** Without providing layer embeddings to L3RS, the optimizer would have more difficulty identifying which layer it was operating on needing to rely heavily on the adaptive EMA features. An alternative to the layer embeddings is to meta-learn a separate MLP model for each layer of the target model. This strategy greatly increases the total parameter count of the optimizer. We investigate both the per-layer MLP style, as well as the single MLP without layer embeddings. See Table 2 for results.

**Ablation of Adaptive EMA Input Features.** We additionally train models with different adaptive EMA feature smoothing factors. While L3RS uses  $\gamma \in \{0.99, 0.9, 0.0\}$ , we also test  $\gamma \in \{0.9, 0.0\}$ ,  $\gamma \in \{0.0\}$  (which corresponds to the raw features without averaging), and  $\gamma \in \emptyset$  (which corresponds to not receiving the adaptive features at all). See Table 3 for results.

**New Directions.** Our main results are based on L3RS which uses only SGD and Adam as given directions. There is a lot of room for exploration in which optimizers and combinations will result in the most powerful L3RS variant for a given task. As an example of the flexibility of the architecture we explore a few combinations here. We leverage the following optimizers: LION (Chen et al., 2023), LAMB (You et al., 2020), ADAMAX (Kingma & Ba, 2014), as well as a WeightDecay direction which

Base Optimizer Set	Accuracy
SGD, ADAM	<b>68.93 ± 4.58</b>
ADAM, LION, LAMB	68.61 ± 4.50
ADAMAX, SGD, LAMB	66.95 ± 4.80
SGD, ADAM, ADAMAX, LION, LAMB, WeightDecay	68.41 ± 4.65

Table 4: Average eval accuracy and standard deviation of L3RS variants, each using a different set of base-optimizers.

simply provides the negative direction of the current parameters. We use the same training/evaluation set up as the rest of the ablations and variants. We report the results in Table 4.

## 7 Conclusions

Learned optimization is a powerful paradigm which has the potential to outperform existing methods. Our results suggest that narrowing the domain that learned optimizers are meta-trained on can provide a reduced meta-training cost, and allow learning domain specific exploitations that can increase their performance, especially on fine-tuning tasks. We provide results repurposing VELO, an architecture designed for general learned optimization, as well as propose a new architecture L3RS, designed to take advantage of the narrow domain. We also demonstrate the robustness of this method on out of distribution tasks. As fine-tuning tasks continue to become more relevant, especially for LLMs, this paradigm and architecture provides a promising direction for future research. Improving this technique further can result in faster model training, better performance, and robust data generalization.

## References

Naman Agarwal, Rohan Anil, Elad Hazan, Tomer Koren, and Cyril Zhang. Learning rate grafting: Transferability of optimizer tuning, 2022. URL [https://openreview.net/forum?id=FpKgG31Z\\_i9](https://openreview.net/forum?id=FpKgG31Z_i9).

Diogo Almeida, Clemens Winter, Jie Tang, and Wojciech Zaremba. A generalizable approach to learning optimizers. *arXiv preprint arXiv:2106.00958*, 2021.

Marcin Andrychowicz, Misha Denil, Sergio Gomez, Matthew W Hoffman, David Pfau, Tom Schaul, Brendan Shillingford, and Nando De Freitas. Learning to learn by gradient descent by gradient descent. *Advances in neural information processing systems*, 29, 2016.

Atilim Gunes Baydin, Robert Cornish, David Martinez Rubio, Mark Schmidt, and Frank Wood. Online learning rate adaptation with hypergradient descent. *arXiv preprint arXiv:1703.04782*, 2017.

Irwan Bello, Barret Zoph, Vijay Vasudevan, and Quoc V Le. Neural optimizer search with reinforcement learning. In *International Conference on Machine Learning*, pp. 459–468. PMLR, 2017.

Samy Bengio, Yoshua Bengio, Jocelyn Cloutier, and Jan Gecsei. On the optimization of a synaptic learning rule. In *Preprints Conf. Optimality in Artificial and Biological Neural Networks*, volume 2, 2013.

Yoshua Bengio, Samy Bengio, and Jocelyn Cloutier. *Learning a synaptic learning rule*. Citeseer, 1990.

Xiangning Chen, Chen Liang, Da Huang, Esteban Real, Kaiyuan Wang, Yao Liu, Hieu Pham, Xuanyi Dong, Thang Luong, Cho-Jui Hsieh, et al. Symbolic discovery of optimization algorithms. *arXiv preprint arXiv:2302.06675*, 2023.

Yutian Chen, Xingyou Song, Chansoo Lee, Zi Wang, Richard Zhang, David Dohan, Kazuya Kawakami, Greg Kochanski, Arnaud Doucet, Marc'aurelio Ranzato, et al. Towards learning universal hyperparameter optimizers with transformers. *Advances in Neural Information Processing Systems*, 35:32053–32068, 2022.

Dami Choi, Christopher J Shallue, Zachary Nado, Jaehoon Lee, Chris J Maddison, and George E Dahl. On empirical comparisons of optimizers for deep learning. *arXiv preprint arXiv:1910.05446*, 2019.

Christian Daniel, Jonathan Taylor, and Sebastian Nowozin. Learning step size controllers for robust neural network training. In *Proceedings of the AAAI Conference on Artificial Intelligence*, volume 30, 2016.

Chelsea Finn, Pieter Abbeel, and Sergey Levine. Model-agnostic meta-learning for fast adaptation of deep networks. In *International conference on machine learning*, pp. 1126–1135. PMLR, 2017.

Riccardo Grazzi, Luca Franceschi, Massimiliano Pontil, and Saverio Salzo. On the iteration complexity of hypergradient computation. In *International Conference on Machine Learning*, pp. 3748–3758. PMLR, 2020.

Vineet Gupta, Tomer Koren, and Yoram Singer. Shampoo: Preconditioned stochastic tensor optimization. In *International Conference on Machine Learning*, pp. 1842–1850. PMLR, 2018.

David Ha, Andrew Dai, and Quoc V. Le. Hypernetworks, 2016.

James Harrison, Luke Metz, and Jascha Sohl-Dickstein. A closer look at learned optimization: Stability, robustness, and inductive biases. *Advances in Neural Information Processing Systems*, 35:3758–3773, 2022.

Pavel Izmailov, Dmitrii Podoprikhin, Timur Garipov, Dmitry Vetrov, and Andrew Gordon Wilson. Averaging weights leads to wider optima and better generalization. *arXiv preprint arXiv:1803.05407*, 2018.

Deepali Jain, Krzysztof M Choromanski, Kumar Avinava Dubey, Sumeet Singh, Vikas Sindhwani, Tingnan Zhang, and Jie Tan. Mnemosyne: Learning to train transformers with transformers. *Advances in Neural Information Processing Systems*, 36, 2024.

Diederik P Kingma and Jimmy Ba. Adam: A method for stochastic optimization. *arXiv preprint arXiv:1412.6980*, 2014.

Günter Klambauer, Thomas Unterthiner, Andreas Mayr, and Sepp Hochreiter. Self-normalizing neural networks, 2017.

Nicola Landro, Ignazio Gallo, and Riccardo La Grassa. Combining optimization methods using an adaptive meta optimizer. *Algorithms*, 14(6):186, 2021.

Ke Li and Jitendra Malik. Learning to optimize. *arXiv preprint arXiv:1606.01885*, 2016.

Kaifeng Lv, Shunhua Jiang, and Jian Li. Learning gradient descent: Better generalization and longer horizons. In *International Conference on Machine Learning*, pp. 2247–2255. PMLR, 2017.

Alejandro López-Cifuentes, Marcos Escudero-Viñolo, Jesús Bescós, and Álvaro García-Martín. Semantic-aware scene recognition. *Pattern Recognition*, 102:107256, June 2020. ISSN 0031-3203. doi: 10.1016/j.patcog.2020.107256. URL <http://dx.doi.org/10.1016/j.patcog.2020.107256>.

Dougal Maclaurin, David Duvenaud, and Ryan Adams. Gradient-based hyperparameter optimization through reversible learning. In *International conference on machine learning*, pp. 2113–2122. PMLR, 2015.

James Martens and Roger Grosse. Optimizing neural networks with kronecker-factored approximate curvature. In *International conference on machine learning*, pp. 2408–2417. PMLR, 2015.

Luke Metz, Niru Maheswaranathan, C Daniel Freeman, Ben Poole, and Jascha Sohl-Dickstein. Tasks, stability, architecture, and compute: Training more effective learned optimizers, and using them to train themselves. *arXiv preprint arXiv:2009.11243*, 2020a.

Luke Metz, Niru Maheswaranathan, Ruoxi Sun, C Daniel Freeman, Ben Poole, and Jascha Sohl-Dickstein. Using a thousand optimization tasks to learn hyperparameter search strategies. *arXiv preprint arXiv:2002.11887*, 2020b.

Luke Metz, C Daniel Freeman, Samuel S Schoenholz, and Tal Kachman. Gradients are not all you need. *arXiv preprint arXiv:2111.05803*, 2021.

Luke Metz, James Harrison, C Daniel Freeman, Amil Merchant, Lucas Beyer, James Bradbury, Naman Agrawal, Ben Poole, Igor Mordatch, Adam Roberts, et al. Velo: Training versatile learned optimizers by scaling up. *arXiv preprint arXiv:2211.09760*, 2022.

Ted Moskovitz, Rui Wang, Janice Lan, Sanyam Kapoor, Thomas Miconi, Jason Yosinski, and Aditya Rawal. First-order preconditioning via hypergradient descent. *arXiv preprint arXiv:1910.08461*, 2019.

Abhinav Moudgil, Boris Knyazev, Guillaume Lajoie, and Eugene Belilovsky. Learning to optimize with recurrent hierarchical transformers. In *ICML Workshop on New Frontiers in Learning, Control, and Dynamical Systems*, 2023.

Isabeau Prémont-Schwarz, Jaroslav Vítku, and Jan Feyereisl. A simple guard for learned optimizers. *arXiv preprint arXiv:2201.12426*, 2022.

Tim Salimans, Jonathan Ho, Xi Chen, Szymon Sidor, and Ilya Sutskever. Evolution strategies as a scalable alternative to reinforcement learning, 2017.

Mark Sandler, Max Vladymyrov, Andrey Zhmoginov, Nolan Miller, Tom Madams, Andrew Jackson, and Blaise Agüera Y Arcas. Meta-learning bidirectional update rules. In *International Conference on Machine Learning*, pp. 9288–9300. PMLR, 2021.

Jürgen Schmidhuber. *Evolutionary principles in self-referential learning, or on learning how to learn: the meta-meta-... hook*. PhD thesis, Technische Universität München, 1987.

Robin M Schmidt, Frank Schneider, and Philipp Hennig. Descending through a crowded valley-benchmarking deep learning optimizers. In *International Conference on Machine Learning*, pp. 9367–9376. PMLR, 2021.

Amirreza Shaban, Ching-An Cheng, Nathan Hatch, and Byron Boots. Truncated back-propagation for bilevel optimization. In *The 22nd International Conference on Artificial Intelligence and Statistics*, pp. 1723–1732. PMLR, 2019.

Antti Tarvainen and Harri Valpola. Mean teachers are better role models: Weight-averaged consistency targets improve semi-supervised deep learning results. *Advances in neural information processing systems*, 30, 2017.

Ruochen Wang, Yuanhao Xiong, Minhao Cheng, and Cho-Jui Hsieh. Efficient non-parametric optimizer search for diverse tasks. *Advances in Neural Information Processing Systems*, 35: 30554–30568, 2022.

Jason Wei, Maarten Bosma, Vincent Y Zhao, Kelvin Guu, Adams Wei Yu, Brian Lester, Nan Du, Andrew M Dai, and Quoc V Le. Finetuned language models are zero-shot learners. *arXiv preprint arXiv:2109.01652*, 2021.

Olga Wichrowska, Niru Maheswaranathan, Matthew W Hoffman, Sergio Gomez Colmenarejo, Misha Denil, Nando Freitas, and Jascha Sohl-Dickstein. Learned optimizers that scale and generalize. In *International conference on machine learning*, pp. 3751–3760. PMLR, 2017.

Yuhuai Wu, Mengye Ren, Renjie Liao, and Roger Grosse. Understanding short-horizon bias in stochastic meta-optimization. *arXiv preprint arXiv:1803.02021*, 2018.

Chang Xu, Tao Qin, Gang Wang, and Tie-Yan Liu. Reinforcement learning for learning rate control. *arXiv preprint arXiv:1705.11159*, 2017.

Zhen Xu, Andrew M Dai, Jonas Kemp, and Luke Metz. Learning an adaptive learning rate schedule. *arXiv preprint arXiv:1909.09712*, 2019.

Yang You, Jing Li, Sashank Reddi, Jonathan Hseu, Sanjiv Kumar, Srinadh Bhojanapalli, Xiaodan Song, James Demmel, Kurt Keutzer, and Cho-Jui Hsieh. Large batch optimization for deep learning: Training bert in 76 minutes, 2020.

Wenqing Zheng, Tianlong Chen, Ting-Kuei Hu, and Zhangyang Wang. Symbolic learning to optimize: Towards interpretability and scalability. *arXiv preprint arXiv:2203.06578*, 2022.

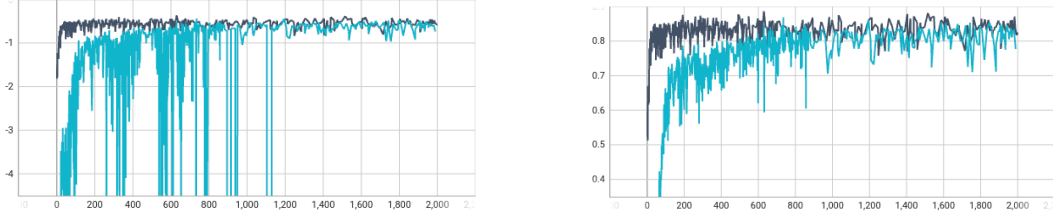


Figure 5: Meta-training curves for L3RS (Black), and VELO (Blue). Left: Average population fitness. Right: Average population evaluation accuracy.

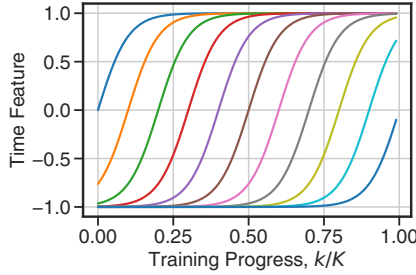


Figure 6: Relative time features as a function of training progress ( $k/K$ ). Each of the lines represents a time input feature to the model, generated using  $k$ ,  $K$ , and  $\alpha_i$ .

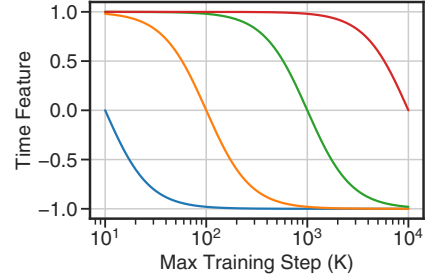


Figure 7: Absolute time features as a function of max training step ( $K$ ). Each of the lines represents a time input feature to the model, generated using  $K$  and  $\beta_j$ .

## A Checkpoint Pretraining

We create the pretrain checkpoints for both IMAGENET and PLACES using the same hyperparameters. We train the models using batch size 128 and train for 100,000 steps. Augmentations/preprocessing used include random cropping to size 224, random mirror, resize, and normalization (based on Imagenet train statistics). For the IMAGENET checkpoint trained on the first 500 classes, we reach an evaluation loss of 0.9387 and an evaluation accuracy of 75.68. For the PLACES checkpoint trained on the first 150 classes, we reach an evaluation loss of 1.312 and an evaluation accuracy of 61.72.

## B Meta-Training

We provide the meta-training curves, both fitness and accuracy, for the two meta-trained learned optimizers. Figure 5 shows the curves for L3RS and VELO throughout training. VELO training is very unstable in this setup, though does converge by the end of training. L3RS reaches a high fitness very rapidly then slowly improves throughout the rest of the training, likely due to the smaller number of parameters in the learned optimizer.

Figures 6 and 7 show the example of the relative and absolute time features used by L3RS.

## C Evaluation Tables

We provide the full evaluation tables from the main evaluation experiments Figure 5 A-E. Table 5 provides the results from the in-domain evaluation A. Table 6 provides the results for all head-only fine-tuning for evaluation A. Table 7 provides the results from the dataset-generalization evaluation B. Table 8 provides the results from the checkpoint-generalization evaluation C. Table 9 provides the results from the initialization and dataset-generalization evaluation D. Table 10 provides the results from the RandomInit evaluation E.

Optimizer	10-Step	25-Step	50-Step	100-Step	250-Step	500-Step	1000-Step	2500-Step
L3RS	68.52 $\pm$ 4.46	76.78 $\pm$ 3.83	80.22 $\pm$ 3.45	83.54 $\pm$ 2.99	86.57 $\pm$ 2.77	88.47 $\pm$ 2.64	88.79 $\pm$ 2.57	89.44 $\pm$ 2.52
VeLO (ft)	62.11 $\pm$ 5.51	73.23 $\pm$ 4.29	77.41 $\pm$ 3.44	81.54 $\pm$ 3.46	85.16 $\pm$ 2.93	86.64 $\pm$ 3.1	73.64 $\pm$ 26.26	4.0 $\pm$ 0.17
VeLO (og)	50.63 $\pm$ 4.9	47.48 $\pm$ 5.2	53.7 $\pm$ 4.6	60.79 $\pm$ 4.24	71.02 $\pm$ 4.08	78.09 $\pm$ 3.62	82.45 $\pm$ 3.19	83.39 $\pm$ 3.04
Adam (cosine), 1e-3	55.86 $\pm$ 4.92	66.38 $\pm$ 4.7	71.03 $\pm$ 4.11	76.59 $\pm$ 4.19	82.53 $\pm$ 3.46	85.34 $\pm$ 3.17	86.84 $\pm$ 2.7	87.25 $\pm$ 2.88
Adam (cosine), 1e-4	10.69 $\pm$ 2.52	28.22 $\pm$ 4.03	52.11 $\pm$ 5.04	70.29 $\pm$ 4.6	81.22 $\pm$ 3.43	85.3 $\pm$ 3.22	87.52 $\pm$ 2.96	88.88 $\pm$ 2.59
Adam (cosine), 1e-5	4.32 $\pm$ 1.45	5.09 $\pm$ 1.62	6.47 $\pm$ 1.81	10.66 $\pm$ 2.29	29.4 $\pm$ 4.0	54.18 $\pm$ 5.05	72.22 $\pm$ 4.67	82.36 $\pm$ 3.52
Adam (const), 1e-3	60.12 $\pm$ 4.62	62.65 $\pm$ 4.37	65.82 $\pm$ 4.24	70.85 $\pm$ 4.23	75.92 $\pm$ 3.94	79.11 $\pm$ 3.7	80.87 $\pm$ 3.58	81.92 $\pm$ 3.61
Adam (const), 1e-4	22.09 $\pm$ 3.54	51.72 $\pm$ 4.98	69.72 $\pm$ 4.59	78.58 $\pm$ 3.95	84.02 $\pm$ 3.07	86.65 $\pm$ 2.93	87.72 $\pm$ 2.76	87.95 $\pm$ 2.78
Adam (const), 1e-5	4.83 $\pm$ 1.56	6.47 $\pm$ 1.77	10.7 $\pm$ 2.29	22.66 $\pm$ 3.62	53.91 $\pm$ 4.99	72.15 $\pm$ 4.6	80.34 $\pm$ 3.62	85.62 $\pm$ 3.16

Table 5: Average and standard deviation evaluation accuracy for main experiment (A).

Optimizer	10-Step	25-Step	50-Step	100-Step	250-Step	500-Step	1000-Step	2500-Step
VeLO (og)	42.53 $\pm$ 4.73	67.93 $\pm$ 4.4	73.68 $\pm$ 3.65	76.35 $\pm$ 3.58	79.12 $\pm$ 3.45	80.71 $\pm$ 3.2	81.36 $\pm$ 3.11	81.6 $\pm$ 3.23
Adam (cosine), 1e-3	7.98 $\pm$ 2.16	16.93 $\pm$ 3.14	34.58 $\pm$ 4.39	54.65 $\pm$ 5.05	69.84 $\pm$ 4.55	74.95 $\pm$ 4.0	78.0 $\pm$ 3.68	80.52 $\pm$ 3.41
Adam (cosine), 1e-4	4.18 $\pm$ 1.47	4.53 $\pm$ 1.59	5.32 $\pm$ 1.7	7.52 $\pm$ 2.06	16.86 $\pm$ 3.24	34.34 $\pm$ 4.53	54.8 $\pm$ 4.99	70.14 $\pm$ 4.72
Adam (cosine), 1e-5	3.95 $\pm$ 1.38	3.98 $\pm$ 1.38	4.05 $\pm$ 1.39	4.21 $\pm$ 1.45	4.55 $\pm$ 1.54	5.24 $\pm$ 1.55	7.32 $\pm$ 1.96	16.74 $\pm$ 3.15
Adam (const), 1e-3	13.31 $\pm$ 2.71	33.5 $\pm$ 4.31	53.59 $\pm$ 4.81	65.91 $\pm$ 4.67	74.17 $\pm$ 4.07	77.34 $\pm$ 3.67	79.53 $\pm$ 3.51	81.17 $\pm$ 3.45
Adam (const), 1e-4	4.44 $\pm$ 1.51	5.22 $\pm$ 1.59	7.4 $\pm$ 1.97	13.27 $\pm$ 3.03	34.17 $\pm$ 4.59	54.5 $\pm$ 4.94	67.28 $\pm$ 4.72	75.17 $\pm$ 3.93
Adam (const), 1e-5	3.98 $\pm$ 1.38	4.01 $\pm$ 1.41	4.21 $\pm$ 1.43	4.43 $\pm$ 1.52	5.22 $\pm$ 1.57	7.32 $\pm$ 2.0	13.13 $\pm$ 3.05	34.35 $\pm$ 4.57

Table 6: Average and standard deviation evaluation accuracy for all Head-only fine-tuning from main experiment (A).

Optimizer	10-Step	25-Step	50-Step	100-Step	250-Step	500-Step	1000-Step	2500-Step
L3RS	59.2 $\pm$ 3.87	69.16 $\pm$ 3.32	73.64 $\pm$ 3.23	76.75 $\pm$ 3.32	80.67 $\pm$ 3.07	82.74 $\pm$ 2.92	84.32 $\pm$ 2.82	85.51 $\pm$ 2.81
VeLO (ft)	50.13 $\pm$ 7.32	64.78 $\pm$ 3.46	70.46 $\pm$ 3.29	74.1 $\pm$ 7.83	79.12 $\pm$ 3.21	76.54 $\pm$ 12.9	56.13 $\pm$ 30.47	4.02 $\pm$ 0.36
VeLO (og)	43.13 $\pm$ 3.98	44.58 $\pm$ 4.18	51.26 $\pm$ 4.18	59.02 $\pm$ 4.0	68.38 $\pm$ 3.83	75.14 $\pm$ 3.47	79.97 $\pm$ 3.49	83.07 $\pm$ 3.13
Adam (cosine), 1e-3	48.85 $\pm$ 3.79	60.39 $\pm$ 3.34	66.11 $\pm$ 3.59	71.81 $\pm$ 3.64	77.71 $\pm$ 3.44	80.73 $\pm$ 3.17	82.99 $\pm$ 2.96	84.97 $\pm$ 2.76
Adam (cosine), 1e-4	9.87 $\pm$ 2.24	23.3 $\pm$ 2.97	44.16 $\pm$ 3.99	63.11 $\pm$ 3.72	74.9 $\pm$ 3.65	79.71 $\pm$ 3.0	82.68 $\pm$ 3.04	85.17 $\pm$ 2.98
Adam (cosine), 1e-5	4.38 $\pm$ 1.53	4.98 $\pm$ 1.55	6.07 $\pm$ 1.68	9.06 $\pm$ 2.06	22.83 $\pm$ 3.06	45.84 $\pm$ 3.56	65.3 $\pm$ 3.72	76.39 $\pm$ 3.54
Adam (const), 1e-3	52.54 $\pm$ 4.3	56.19 $\pm$ 3.93	61.15 $\pm$ 3.92	65.87 $\pm$ 3.94	71.71 $\pm$ 3.52	74.83 $\pm$ 3.42	77.42 $\pm$ 3.57	80.51 $\pm$ 3.28
Adam (const), 1e-4	17.32 $\pm$ 2.81	43.3 $\pm$ 3.74	62.03 $\pm$ 3.48	71.65 $\pm$ 3.48	78.01 $\pm$ 3.28	80.57 $\pm$ 2.85	82.72 $\pm$ 3.01	84.66 $\pm$ 2.97
Adam (const), 1e-5	4.73 $\pm$ 1.54	6.08 $\pm$ 1.66	9.05 $\pm$ 2.15	17.72 $\pm$ 2.64	45.84 $\pm$ 3.79	64.93 $\pm$ 3.85	74.3 $\pm$ 3.65	80.72 $\pm$ 3.3

Table 7: Average and standard deviation evaluation accuracy for main experiment (B).

Optimizer	10-Step	25-Step	50-Step	100-Step	250-Step	500-Step	1000-Step	2500-Step
L3RS	65.65 $\pm$ 4.61	73.13 $\pm$ 3.99	77.0 $\pm$ 4.02	80.33 $\pm$ 3.59	83.79 $\pm$ 3.06	85.93 $\pm$ 2.97	86.91 $\pm$ 2.78	87.04 $\pm$ 2.68
VeLO (ft)	57.85 $\pm$ 7.39	69.6 $\pm$ 4.0	73.51 $\pm$ 4.09	77.96 $\pm$ 3.8	82.18 $\pm$ 3.22	84.46 $\pm$ 2.95	82.67 $\pm$ 11.37	4.04 $\pm$ 0.27
VeLO (og)	52.35 $\pm$ 4.67	49.56 $\pm$ 4.78	54.52 $\pm$ 4.72	61.44 $\pm$ 4.58	71.37 $\pm$ 4.1	77.87 $\pm$ 3.67	81.7 $\pm$ 3.15	82.82 $\pm$ 3.08
Adam (cosine), 1e-3	55.36 $\pm$ 4.8	62.93 $\pm$ 4.44	67.45 $\pm$ 4.35	72.54 $\pm$ 4.18	79.14 $\pm$ 3.41	82.61 $\pm$ 3.09	84.43 $\pm$ 3.19	85.36 $\pm$ 3.17
Adam (cosine), 1e-4	13.27 $\pm$ 2.7	33.25 $\pm$ 4.39	54.11 $\pm$ 4.84	68.21 $\pm$ 4.46	78.83 $\pm$ 3.61	83.49 $\pm$ 3.16	85.96 $\pm$ 2.98	87.31 $\pm$ 2.66
Adam (cosine), 1e-5	4.37 $\pm$ 1.52	5.26 $\pm$ 1.72	7.14 $\pm$ 2.02	12.29 $\pm$ 2.7	33.43 $\pm$ 4.16	56.37 $\pm$ 4.73	70.46 $\pm$ 4.56	80.28 $\pm$ 3.51
Adam (const), 1e-3	56.2 $\pm$ 4.9	58.38 $\pm$ 4.31	61.7 $\pm$ 4.4	66.41 $\pm$ 4.45	72.24 $\pm$ 4.05	75.95 $\pm$ 3.68	78.45 $\pm$ 3.38	80.04 $\pm$ 3.6
Adam (const), 1e-4	25.4 $\pm$ 3.79	53.72 $\pm$ 4.75	67.04 $\pm$ 4.56	75.64 $\pm$ 4.01	81.56 $\pm$ 3.42	84.25 $\pm$ 3.09	85.96 $\pm$ 2.8	85.92 $\pm$ 2.75
Adam (const), 1e-5	4.87 $\pm$ 1.58	6.97 $\pm$ 2.01	12.38 $\pm$ 2.59	26.29 $\pm$ 4.03	56.09 $\pm$ 4.69	70.48 $\pm$ 4.56	78.41 $\pm$ 3.75	83.96 $\pm$ 3.11

Table 8: Average and standard deviation evaluation accuracy for main experiment (C).

Optimizer	10-Step	25-Step	50-Step	100-Step	250-Step	500-Step	1000-Step	2500-Step
L3RS	72.15 $\pm$ 3.71	77.52 $\pm$ 3.11	80.22 $\pm$ 3.35	81.76 $\pm$ 3.27	83.89 $\pm$ 3.0	84.96 $\pm$ 2.81	85.95 $\pm$ 2.83	87.06 $\pm$ 2.79
VeLO (ft)	66.93 $\pm$ 7.24	75.68 $\pm$ 3.35	78.26 $\pm$ 3.38	80.88 $\pm$ 2.98	83.33 $\pm$ 3.06	80.12 $\pm$ 12.15	59.12 $\pm$ 30.85	4.05 $\pm$ 0.37
VeLO (og)	58.38 $\pm$ 4.31	54.52 $\pm$ 3.97	58.73 $\pm$ 4.2	64.48 $\pm$ 3.83	73.04 $\pm$ 3.49	78.45 $\pm$ 3.33	81.84 $\pm$ 3.41	84.44 $\pm$ 2.41
Adam (cosine), 1e-3	60.65 $\pm$ 4.08	67.66 $\pm$ 3.13	70.77 $\pm$ 3.74	74.73 $\pm$ 3.69	79.2 $\pm$ 3.24	81.41 $\pm$ 3.25	83.47 $\pm$ 3.13	85.58 $\pm$ 3.78
Adam (cosine), 1e-4	15.17 $\pm$ 2.9	38.45 $\pm$ 4.37	61.08 $\pm$ 3.91	74.22 $\pm$ 3.33	80.98 $\pm$ 3.45	83.73 $\pm$ 3.03	85.26 $\pm$ 3.0	86.8 $\pm$ 2.98
Adam (cosine), 1e-5	4.86 $\pm$ 1.84	5.88 $\pm$ 2.0	7.95 $\pm$ 2.25	13.78 $\pm$ 3.02	38.75 $\pm$ 4.17	63.86 $\pm$ 3.64	76.06 $\pm$ 3.29	82.1 $\pm$ 2.81
Adam (const), 1e-3	60.29 $\pm$ 4.24	60.9 $\pm$ 3.63	63.8 $\pm$ 3.57	68.15 $\pm$ 3.88	72.46 $\pm$ 3.92	75.25 $\pm$ 3.52	77.68 $\pm$ 3.61	80.7 $\pm$ 3.14
Adam (const), 1e-4	29.37 $\pm$ 4.04	60.46 $\pm$ 3.96	73.09 $\pm$ 3.48	78.62 $\pm$ 3.34	81.95 $\pm$ 3.29	83.27 $\pm$ 2.93	84.38 $\pm$ 2.99	85.86 $\pm$ 2.64
Adam (const), 1e-5	5.43 $\pm$ 1.9	7.8 $\pm$ 2.26	13.8 $\pm$ 2.96	30.14 $\pm$ 4.13	63.53 $\pm$ 3.66	75.85 $\pm$ 3.25	80.89 $\pm$ 3.24	84.49 $\pm$ 3.66

Table 9: Average and standard deviation evaluation accuracy for main experiment (**D**).

Optimizer	10-Step	25-Step	50-Step	100-Step	250-Step	500-Step	1000-Step	2500-Step
L3RS	15.77 $\pm$ 2.99	21.11 $\pm$ 3.52	25.5 $\pm$ 3.88	30.46 $\pm$ 4.05	40.32 $\pm$ 4.33	47.69 $\pm$ 4.26	54.74 $\pm$ 4.09	60.9 $\pm$ 4.04
VeLO (ft)	16.18 $\pm$ 3.69	18.59 $\pm$ 3.27	18.55 $\pm$ 6.33	11.59 $\pm$ 8.62	5.49 $\pm$ 5.06	7.87 $\pm$ 7.24	4.38 $\pm$ 0.98	3.98 $\pm$ 0.27
VeLO (og)	17.69 $\pm$ 3.1	21.04 $\pm$ 3.66	24.83 $\pm$ 3.72	30.11 $\pm$ 4.28	42.68 $\pm$ 4.34	53.73 $\pm$ 3.87	64.06 $\pm$ 4.14	73.21 $\pm$ 3.92
Adam (cosine), 1e-3	14.48 $\pm$ 2.49	19.26 $\pm$ 3.13	23.45 $\pm$ 3.71	28.14 $\pm$ 3.71	38.59 $\pm$ 4.42	46.64 $\pm$ 4.2	55.25 $\pm$ 4.19	66.46 $\pm$ 3.88
Adam (cosine), 1e-4	5.02 $\pm$ 1.43	7.46 $\pm$ 1.92	12.07 $\pm$ 2.49	17.92 $\pm$ 3.09	24.83 $\pm$ 3.62	32.58 $\pm$ 4.26	43.25 $\pm$ 4.41	56.57 $\pm$ 3.98
Adam (cosine), 1e-5	4.17 $\pm$ 1.18	4.29 $\pm$ 1.2	4.46 $\pm$ 1.25	4.97 $\pm$ 1.35	7.2 $\pm$ 1.96	12.18 $\pm$ 2.64	18.75 $\pm$ 3.21	26.31 $\pm$ 3.67
Adam (const), 1e-3	17.19 $\pm$ 3.05	20.19 $\pm$ 3.34	23.95 $\pm$ 3.68	28.74 $\pm$ 4.2	37.17 $\pm$ 4.62	44.95 $\pm$ 4.21	53.75 $\pm$ 4.12	65.26 $\pm$ 3.64
Adam (const), 1e-4	6.34 $\pm$ 1.72	12.18 $\pm$ 2.62	17.68 $\pm$ 2.95	22.36 $\pm$ 3.41	30.64 $\pm$ 4.12	40.09 $\pm$ 4.14	48.52 $\pm$ 4.22	59.35 $\pm$ 4.15
Adam (const), 1e-5	4.24 $\pm$ 1.23	4.43 $\pm$ 1.24	4.95 $\pm$ 1.38	6.37 $\pm$ 1.64	12.21 $\pm$ 2.6	18.84 $\pm$ 3.19	24.37 $\pm$ 3.61	34.44 $\pm$ 4.33

Table 10: Average and standard deviation evaluation accuracy for main experiment (**E**).